Microchim Acta (2017) 184:3799–3808
DOI 10.1007/s00604-017-2404-z

ORIGINAL PAPER

Organo-silica hybrid capillary monolithic column with mesoporous silica particles for separation of small aromatic molecules

Anica Weller[1] · Enrique Javier Carrasco-Correa[1] · Carolina Belenguer-Sapiña[1] · Adela de los Reyes Mauri-Aucejo[1] · Pedro Amorós[2] · José Manuel Herrero-Martínez[1]

Received: 31 March 2017 / Accepted: 26 June 2017 / Published online: 8 July 2017

Abstract Monolithic stationary phases for use in capillary electrochromatography were prepared by incorporation of mesoporous silica particles (of type MCM-41 or UVM-7) in a polymer obtained from butyl methacrylate and ethylene glycol dimethacrylate as monomers, 1,4-butanediol and 1-propanol as porogen, and azobisisobutyronitrile as initiator. The stability of the dispersions with varying fractions of silica particles was investigated by UV-vis spectrometry. Using continuous stirring during the capillary filling and short UV-polymerization times, polymeric beds with homogenously dispersed mesoporous particles (with contents up to 35 wt% of silica) are obtained. The resulting hybrid monolithic columns were characterized using scanning electron microscopy. The chromatographic performance of these novel stationary phases was evaluated by using alkyl benzenes and benzoic acid derivatives as test analytes. The use of these polymers leads to increased retention and separation efficiency compared to the parent monolith. The column efficiency reached values of up to 140,000 plates m^{-1}. The resulting hybrid monolithic columns also exhibited a satisfactory reproducibility with relative standard deviations of *ca.* 14% (batch-to-batch).

Keywords Polymer monolith · Silica (nano)particles · Hybrid stationary phases · Capillary electrochromatography · High particle contents · Embedded particles

Introduction

In the last years, mesoporous silica particles (MSPs) have gained a lot of attention due to their favorable properties (e.g. mechanical, thermal and chemical stability), low density, good biocompatibility, easy and diverse controlling of particle size and morphologies. These materials have received considerable attention and have been applied to several fields [1–3]. However, we can consider their potential uses in analytical chemistry [4] as laggards when compared to the previous mentioned areas.

The synthesis of MSPs is achieved by using sol-gel technique. Under basic conditions, the silicon precursors condensate in the presence of cationic surfactants. MSPs consist of an amorphous silicon matrix with mesopore sizes ranging from 2 to 50 nm and extremely large surface areas (*ca.* 1000 $m^2\ g^{-1}$). These materials show a mesostructure defined by an ordered and repetitive array of cylindrical mesopores that leads to high pore volumes (>1 $cm^3\ g^{-1}$). Moreover, the mesoporous SPs can be easily functionalized ensuring a suitable design for specific applications [5]. Within the MSP family, MCM-41 is the most studied and applied material. However, lately, other MSPs with different shape and porous systems have been described such as SBA-15 [6–8] and the hierarchical multimodal UVM-7 materials [9–12]. These last MSPs can be described as bimodal porous silicas constructed by aggregation of pseudo-spherical mesoporous primary nanoparticles.

From the preparative point of view, the main difference between UVM-7 and MCM-41 is the less basic conditions employed for its synthesis. Under these conditions, re-

Electronic supplementary material The online version of this article (doi:10.1007/s00604-017-2404-z) contains supplementary material, which is available to authorized users.

✉ José Manuel Herrero-Martínez
jmherrer@uv.es

[1] Department of Analytical Chemistry, University of Valencia, Dr. Moliner 50, 46100 Burjassot, Valencia, Spain

[2] University of Valencia, Institut de Ciència dels Materials, P.O. Box 22085, 46071 Valencia, Spain

dissolution of particles is not favoured and the system generates randomly aggregated structures, which resulted in the bimodal pore system after removal of the surfactant. Thus, UVM-7 has been used in several applications [13]; however, the use of this material in separation field has not been reported.

Polymethacrylate-based monolithic columns are the most widespread and the best characterized columns, being mainly developed by Svec *et al.* [14, 15], and several applications in both, high performance liquid chromatography (HPLC) and capillary electrochromatography (CEC) such as peptides/proteins [16], DNA [17] and chiral compounds [18] have been described. These polymers present several advantages such as easily adjustable polarity, fine control for pore characteristics and high stability under extreme pH conditions (pH 2–12).

In spite of these good features, these macroporous polymeric monoliths have relatively low surfaces areas due to the absence of an adequate micro- or mesoporous structure, which results in reduced sample load capacity and weak retention for chromatographic applications.

In order to overcome this limitation, several strategies have been proposed [15]. In this sense, the approaches consisting of incorporation of nanoparticles to the monoliths have emerged as an effective and promising way of increasing the surface-to-volume ratio, as well as to serve as new platforms to further or more efficiently modify the surface chemistries [19]. Due to their large surface-to-volume ratio, nanomaterials can result in enhanced retention and increased sample loading capacity. These nanostructures can be introduced into the monolith supports by simple entrapment during polymerization or attachment onto pore surface of monolithic matrix.

Thus, the preparation of monolithic structures with embedded nanoparticles such as carbon nanotubes [20, 21] and silver nanoparticles [22] has been described and used as chromatographic supports, giving improved separation efficiency and enhanced chromatographic retention. However, a few studies related to the incorporation of other materials such as MSPs to organic polymers as stationary phases for HPLC and related techniques have been reported [23–25]. In particular, Lei and co-workers [23] have added SBA-15 into methacrylate monoliths for its application in CEC. The selectivity and column efficiency in the resulting hybrid monoliths were greatly enhanced by embedding of these NPs.

Moreover, the effects of nature and size of mesoporous MSPs on hybrid monolithic column and its influence on separation mechanism and retention have not been investigated in detail in previous works. On the other hand, the content of MSPs employed in these studies [23, 24] was limited up to 1 wt%, due to aggregation phenomena of these materials, being a drawback for fully displaying their excellent adsorption capabilities. In this context, the preparation of novel stationary phases with high contents of MSPs combined with the remarkable characteristics of polymeric organic monoliths can be an attractive alternative as chromatographic supports in miniaturized separation techniques.

In this work, novel stationary phases for CEC based on hybrid polymeric monoliths containing MSPs were developed. For this purpose, two different types of these materials with different morphological features, MCM-41 and UVM-7, were chosen for incorporating into the monolithic polymer matrix in order to increase surface area of parent monoliths and to tailor its chromatographic performance. Preparation conditions, including MSPs percentage and dispersion stability, were optimized to avoid sedimentation of MSPs and to improve the separation ability. The hybrid stationary phases were morphologically characterized using SEM and its chromatographic performance was evaluated by using several mixtures of test solutes (alkyl benzenes, derivatives of benzoic acids, cresols and toluene/thiourea) in order to explore the potential enhancement of retention and separation mechanism. Also, the columns were used for the analysis of an analgesic tablet formulation. Finally, the reproducibility in the preparation of hybrid monolithic columns was also evaluated.

Experimental

Materials and methods

Butyl methacrylate (BMA), ethylene dimethacrylate (EDMA), [2-methacryloyloxy)-ethyl]-trimethylammonium chloride (75 wt% in water, META), 1,4-butanediol, 3-(trimethoxysilyl)-propyl methacrylate (MPS), α,α'-azoisobutyronitrile (AIBN) were from Sigma-Aldrich (Milwaukee, WI, USA, http://www.sigmaaldrich.com). 1-Propanol, acetonitrile (ACN), methanol (MeOH) were from Scharlau (Barcelona, Spain, http://www.scharlab.com). Thiourea as an electroosmotic flow (EOF) marker, alkyl benzenes (toluene, ethyl benzene, propyl benzene, butyl benzene, pentyl benzene, and hexyl benzene) were from Riedel de Haën (Seelze, Germany, http://www.riedeldehaen.com/) and benzoic acid derivatives (benzoic (pK_a = 4.2 [26]) and o-phthalic acids (pK_{a1} = 2.94, pK_{a2} = 5.41)), *m*-, *p*- and *o*-cresol were from Acros Organics (Geel, Belgium, http://www.acros.com/), 2-iodobenzoic acid (pK_a = 2.86) from Fluka (Buchs, Switzerland, http://www.sigmaaldrich.com) salicylic acid (pK_a = 2.97), acetylsalicylic acid (pK_a = 3.48) was from Guinama (Valencia, Spain, http://www.guinama.com/). 2,2′,2″-nitriletriethanol (TEAH3), cetyltrimethylammonium bromide (CTAB), tetraethyl orthosilicate (TEOS) were from Sigma-Aldrich. Unless otherwise stated, other chemicals used were of analytical grade. Deionized water was obtained with a Barnstead deionizer (Sybron, Boston, MA, USA).

Fused-silica capillaries (33.5 cm total capillary length, 100 μm ID × 375 μm OD) with UV-transparent coating (Polymicro Technologies, Phoenix, AZ, USA, http://

www.molex.com/molex/products/group?key = polymicro&channel = products) were used. The effective monolithic bed length was 8.5 cm.

Stock solutions of alkyl benzenes, benzoic acid derivatives, toluene and thiourea were prepared in ACN at 1.0 mg mL^{-1} each and kept at 4 °C until use. Working standard solutions were freshly prepared by dilution with the mobile phase.

Aspirin tablets were obtained at a local drugstore. The tablets were powdered and extracted with ethanol:water (20:80 *v*/v) for 1 h in an ultrasonic bath, and the extract was filtered through a 0.45 μm filter and injected into CEC system.

Instrumentation

Transmission electron microscopy (TEM) images of MSPs were obtained using a Jeol (Tokyo, Japan, http://www.jeol.co.jp/en/) model JEM-1010 microscope operated at 100 kV. Surface area, pore size and volume were measured by porosimetry using nitrogen adsorption-desorption isotherms. The isotherms were recorded with a Micrometrics ASAP2020 automated sorption analyzer (http://www.micromeritics.com/). The specific surface areas were calculated from the adsorption data in the low pressure range using the BET model. Pore size was determined following the BJH method. An ultrasonic bath Transsonic digital S (Elma, Germany, http://www.elma-ultrasonic.com/es/), a vortex REAX 2000 (Heidolph, Germany, http://www.heidolph.es/heidolph-instruments/) and a magnetic stirrer ANS-001 (SBS Labscience, Madrid, Spain, http://www.websbs.com/) were employed to disperse silica material (MCM-41 and UVM-7). To photoinitiate polymerization, the capillaries were placed into an UV crosslinker chamber (model CL1000, UVP, Upland, CA, USA, https://www.uvp.com/) equipped with five UV lamps (5 × 8 W, 254 nm). Conditioning steps of the monolithic columns were performed with an HPLC pump 110B Solvent Delivery module (Beckman, Pasadena, CA, USA, https://www.beckmancoulter.com) and L-6200A Intelligent Pump (Merck, Darmstadt, Germany, http://www.merck.es/es/index.html). The sedimentation of dispersions of MSPs in the polymerization mixtures were carried out with UV/VIS-Spectrophotometer with single pulsed xenon lamp (model 6305, Jenway, Staffordshire, UK, http://www.jenway.com/) provided with a 1 mm optical-path quartz cell (Hellma, Müllheim, Germany, http://www.hellma-analytics.com/startseite/1/en/home.html) at 500 nm. SEM photographs of cross section of the hybrid monolithic capillaries were taken (at 20 kV and a working distance of 14 mm) with a scanning electron microscope (S-4800, Hitachi, Ibaraki, Japan, http://www.hitachi.eu/es-es) provided with a field emission gun, an EMIP 3.0 image data acquisition system and a microanalysis system (Rontec, Normanton, UK, http://www.rontec.com/). CEC experiments were performed with an HP3DCE instrument (Agilent Technologies, Waldbronn, Germany, https://www.agilent.com/) with a diode-array UV detector and connected to external nitrogen supply. Data acquisition was performed with the ChemStation Software (Rev.A.10.01, Agilent).

Synthesis of MSPs (MCM-41 and UVM-7)

The method used to prepare both materials, denoted as atrane route, is based on the use of a cationic surfactant (CTAB) as structural directing agent (and, consequently, as porogen after template removal), and a complexing polyalcohol (TEAH3) as hydrolysis retarding agent [9–11]. In both cases, the same molar ratio of the reagents was used: 2Si: 7 TEAH3: 0.5 CTAB: 180 H_2O, and the pH control allow us to synthesize MCM-41 or UVM-7 materials. The details of synthesis of these materials are given in supplementary material.

The synthesis of Gd-UVM-7 material (with a Si/Gd = 25 M ratio) was carried out by using exactly the same protocol described for the UVM-7 silica, and mixing the TEOS and $GdCl_3$ with TEAH3 in the first preparation step. The reagent molar ratio used was 1.92 Si: 0.08 Gd: 7 TEAH3: 0.5 CTAB: 180 H_2O [9].

Preparation of monolithic columns with MSPs

To ensure covalent attachment of the monolithic beds, the modification (vinylization) of the inner fused-silica capillary walls was carried out with MPS according to the literature [27]. Monolithic columns were prepared from a polymerization mixture consisting of BMA (25.5 wt%) EDMA (17.0 wt%), META to generate EOF in CEC (0.4 wt%), and a binary porogenic solvent consisting of 1,4-butanediol (19.0 wt%) and 1-propanol (38.1 wt%) and AIBN (1 wt% with respect to the monomers) was added as initiator. The mixture was sonicated for 15 min in an ultrasonic bath and afterwards purged with nitrogen for 10 min.

Different amounts of MCM-41 or UVM-7 were added to the polymerization mixture to give a final content in the mixtures ranging from 0.5 to 35 wt%. Then, the suspensions were sonicated for 10 min and vortexed for 2 min. To avoid sedimentation processes during capillary filling, the (nano)particle dispersions were stirred throughout the whole time of capillary filling with a syringe pump. The silanized capillary was filled up to a length of 8.5 cm and was polymerized in the UV-crosslinker chamber at 0.9 $J \cdot cm^{-2}$ for 15 min. After polymerization, the resulting columns were flushed with MeOH using an HPLC pump in order to remove the porogenic solvents and non-reacted monomer species. Then, the capillaries were flushed with the mobile phase.

To study the stability of the suspensions of MSPs, the vortexed mixture was filled into a 1 mm optical-path quartz cell and UV-measurements for 60 min were performed. The wavelength was set at 500 nm and the decrease of scattering (apparent absorbance) was monitored.

CEC procedures adopted in this work are described in the Electronic Supporting Material.

Results and discussion

Characterization of MSPs

The morphology of the synthesized MSPs (MCM-41 and UVM-7) was investigated by TEM (Figure S1). As shown in Fig. S1A, the MCM-41 particles display a pseudo-spherical shape and have particle diameters of 245 ± 95 (n = 100) with a wide size distribution (Fig. S1A). These relatively large particles are partially aggregated in the form of clusters. Furthermore, the MCM-41 material shows a high porosity with a partially hexagonal ordered mesostructure. The UVM-7 organization also presents high porosity together with a certain disordered hexagonal mesopore array. However, in this case, the pseudo-spherical nanoparticles (Fig. S1B) with primary particle sizes of 17 ± 5 (n = 100) (Fig. S1B), presented a narrow size distribution.

Furthermore, the surface area and pore-size distribution of the prepared MSPs were characterized by using nitrogen adsorption-desorption isotherms (Figs. S1C and D). In both cases, the curves show one well-defined step at intermediate partial pressures ($0.2 < P/P_0 < 0.5$) characteristic of Type IV isotherms, which should be due to the capillary condensation of N_2 inside the surfactant-generated mesopores. In the case of the UVM-7 silica, an additional adsorption step appears at higher partial pressure values. This second step, at a high relative pressure ($P/P_0 > 0.8$), corresponds to the filling of the large pores among the primary nanoparticles. In this last case, the curves show a characteristic H1 hysteresis loop and a wide pore size distribution. Application of the Barrett-Joyner-Halenda (BJH) model (adsorption branch of the isotherms) estimates large pore size values falling in the limit between meso and macropores (see Table 1). This table summarizes the BET surface areas, the average pore width and the total pore volume for both MSPs from the adsorption-desorption isotherms. Briefly, both materials display a similar intraparticle mesostructure based on the existence of cylindrical mesopores. The relative order of the mesopores seems to be slightly higher in the case of the MCM-41 material. The principal difference between both materials is the size of the silica particles: nanometric or micrometric for UVM-7 and MCM-41, respectively. This difference generates the formation of a second large pore system in the case of the UVM-7 (through aggregation of the primary nanoparticles).

Preparation and characterization of hybrid monolithic columns with MSPs

In order to achieve homogeneous monolithic stationary phases with incorporated MSPs in capillary, it is necessary to uniformly disperse these materials in polymerization mixture. For this purpose, before capillary filling, the combination of ultrasonic bath (10 min) with vortex mixing (1 min) was used to disperse particles. Next, the stability of these dispersions was monitored by light scattering at 500 nm. This wavelength was selected to avoid signal contribution of methacrylate monomers and UV initiating of the polymer (200–280 nm). Also, a polymerization mixture without MSPs was used as blank. The turbidimetric measurements were implemented with a BMA mixture containing contents comprised between 0.5 and 5 wt% for each type of MSPs (MCM-41 or UVM-7) (Fig. S2). As it can be seen, a decrease in the light scattering for both types of MSPs, which implies a sedimentation process was evidenced, being particular more for MCM-41 due to its larger particle size than UVM-7. Although these latter particles showed only a low light scattering, their sedimentation was also perceptible (see Fig. S2B). Since the sedimentation time was lower than the time required for proper capillary filling (approx. 5–15 min) and for UV polymerization (15 min), a stirring step was introduced after dispersion with ultrasonic bath and vortex mixing. In order to evaluate the effect of stirring the polymerization mixture along the capillary filling, blank or control polymerization mixture (without MSPs) were prepared. CEC properties of the resulting monoliths were examined, and no significant differences between the tested stirring rates were evidenced (data not shown). By using this approach, polymerization mixtures containing increasing contents of MSPs were prepared. The highest percentage found for each type (35 and 10 wt% for MCM-41 and UVM-7, respectively) of MSPs was conditioned by the viscosity of the polymerization mixture, which hindered an adequate capillary filling. The use of these large MSP concentrations did not show absorption bands at the selected photoinitiation wavelength (254 nm) (see Fig. S3). Besides, the prepared columns using this methodology provided homogenous monolithic beds (see Fig. 1), and as we shall discuss later, an enhanced retention with increasing MSP contents (see next section). Together with our optimized preparative protocol, we consider that the porosity of the MSPs favor the column homogeneity, and consequently hinders any segregation phenomena when compared with the use of massive silica charges (non-porous silica particles). This effect must be attributed to the lower density of the mesoporous silica which led to a restricted sedimentation.

Additionally, to confirm the regular distribution of (incorporated) MSPs in the polymeric matrices, gadolinium-doped mesoporous silica UVM-7 material was synthesized. The atrane method allows us to introduce a large variety of elements inside the silica framework [9]. The selection of Gd species as local probe is based on the following reasons: i) while others elements (mainly transition metals) are present in low proportion in the silica materials, rare earths as Gd are not frequent and ii) the Gd can be dispersed along the silica material in a very homogeneous way, without segregation as Gd_2O_3 oxides, when the atrane method is used. Moreover, a relatively small amount of Gd was introduced (see

Table 1 BET surface area, average pore width and total pore volume for the synthesized MSPs, MCM-41 and UVM-7

MSP	BET surface area ($m^2\ g^{-1}$)	BJH mesopore size (nm)	BJH large pore size (nm)	Total pore volume ($cm^3\ g^{-1}$)
MCM-41	1256.8	2.41	-	0.76
UVM-7	1034.1	2.91	52.8	1.85

Experimental section) in order to keep unaltered the morphological features of parent silica material. Thus, hybrid monoliths containing large MSP contents (*e.g.* 10 wt% UVM-7) were prepared. Then, the bed of hybrid monolithic capillary (8.5 cm) was cut into 1 cm long pieces, and energy dispersive X-ray analysis (EDAX) on a 20 μm section of monolith near to the center of the support in the different column pieces was performed. EDAX results indicated that the molar ratio Si/Gd gave values close to 24 in the different pieces examined in the same column (see Fig. S4), which confirms the uniformity of prepared composites.

Next, the morphology of the hybrid monolithic columns was studied with SEM. As shown in Fig. 1, the hybrid monoliths containing either MCM-41 or UVM-7 materials (parts B-C) did not show significant changes at 18,000× magnification in the polymer skeleton porous structure compared to BMA columns prepared in absence of MSPs (control monolith, Fig. 1A). This observation is in agreement with that found by Lei *et al.* for hybrid monoliths containing functionalized SBA-15 silica nanoparticles [23]. This suggests that most of MSPs were completely embedded into the poly(BMA-*co*-EDMA) matrix. Nevertheless, the SEM images of monoliths at higher magnification (50,000×) and prepared at large MSP contents showed some differences between the monoliths containing MSPs (Figs. 1E and F) and the control monolith (Fig. 1D). Thus, the monoliths containing MCM-41 (Fig. 1E) showed spherical pellets at the microglobules with sizes fitting reasonably well with those of MCM-41 materials (~ 200 nm). Also, these pellets are homogeneously distributed through the monolith surface. In the case of the monoliths containing UVM-7 nanoparticles (Fig. 1F), no visible changes were evidenced on the surface, although the microglobules showed a rougher aspect than the control column (Fig. 1D).

CEC evaluation of hybrid monolithic columns with MSPs

The CEC performance of the hybrid polymeric monoliths with embedded MSPs as stationary phases was evaluated using different test solutes. Fig. 2 shows the separation of alkyl benzenes using the control BMA-based monolith and hybrid columns containing MCM-41 at several contents (from 2 to 35 wt%). As observed, the retention time for all alkyl benzenes increases progressively with increasing percentages of embedded MCM-41 particles, being higher than those found in control monolith. Also, an increase of retention time of the EOF marker (or a reduction of flow rate, *u*) was evidenced (see Fig. 2 and Table 2). This behavior is attributed to a decrease of the density of the quaternary ammonium functionalities of META (ionizable monomer) on the monolith surface. The reduction of the EOF observed was justified by the dilution produced in the mixture by the presence of large contents of MSPs. These findings were also consistent with other

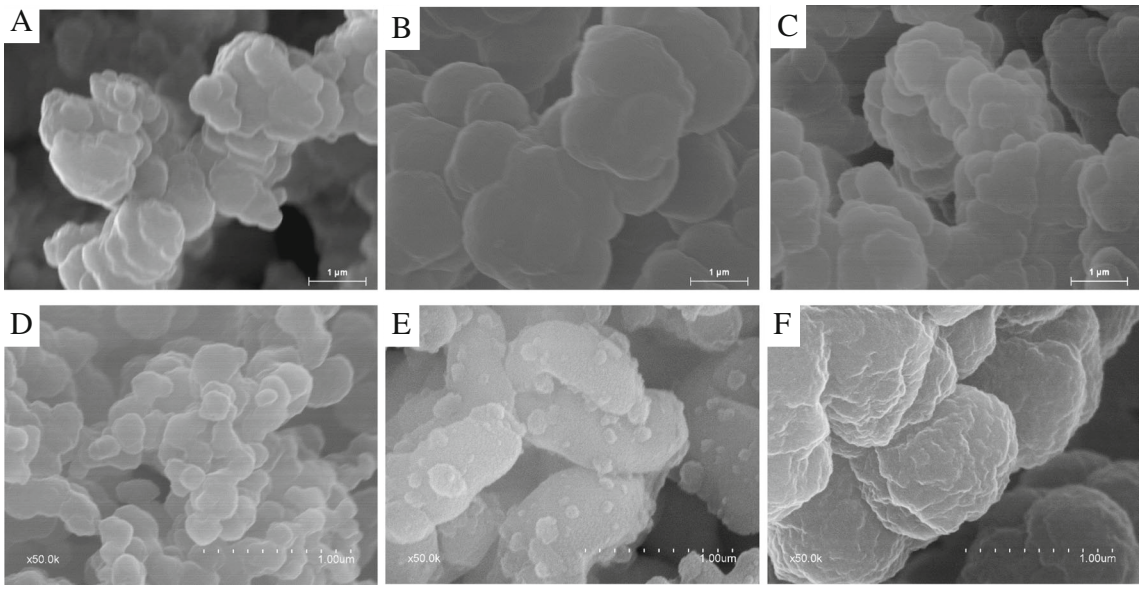

Fig. 1 SEM micrographs of hybrid monolithic columns containing different amounts of MSPs at 18,000×: control monolith (without MSPs) (A); 5 wt% MCM-41 (B); 5 wt% UVM-7 (C); and at 50,000×: control monolith (without MSPs) (D); 35 wt% MCM-41 (E) and 10 wt% UVM-7 (F)

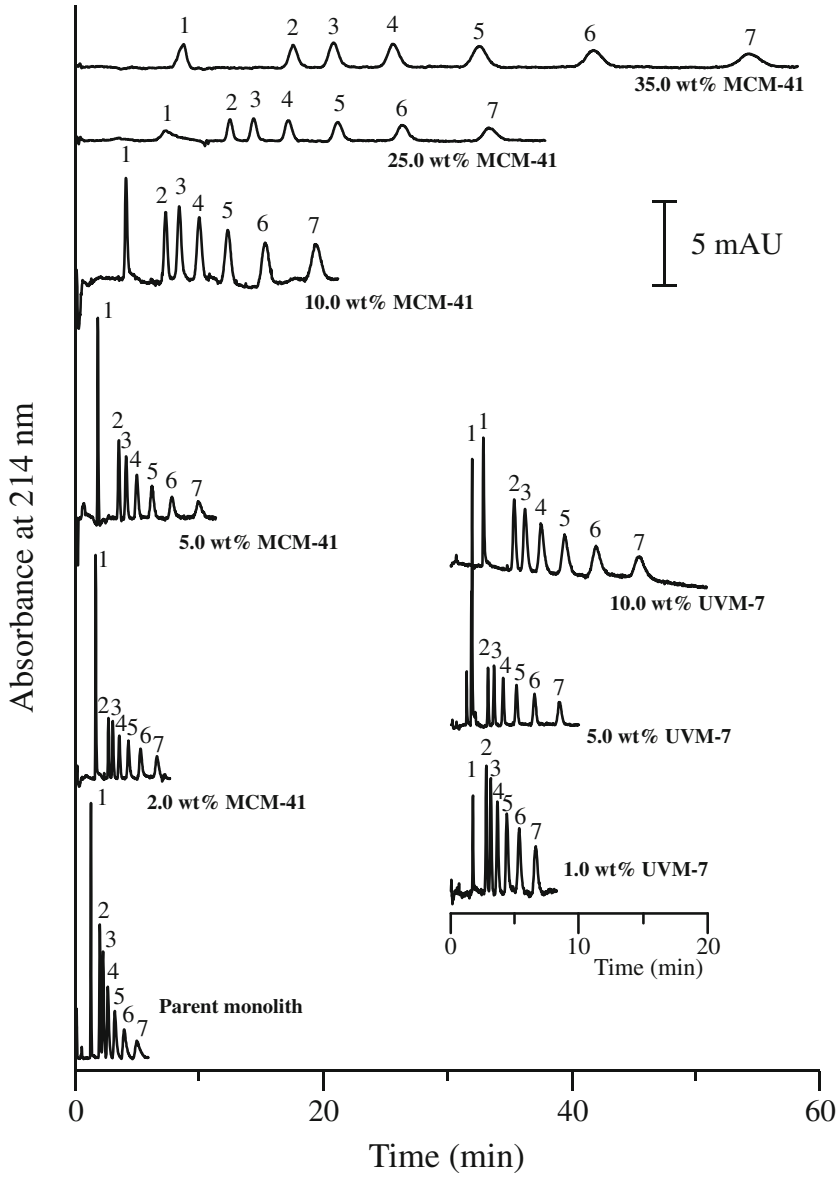

Fig. 2 CEC separation of alkyl benzenes in absence (control monolith) and presence of different amounts of MCM-41 or UVM-7. Experimental conditions: columns: 8.5/33.5 cm × 100 μm; mobile phase, 60:40 ACN:H_2O, 5 mM H_3PO_4, pH = 2.5; injection: 10 kV × 3 s; separation voltage, 25 kV; detection wavelength, 214 nm. Solutes: thiourea (1, EOF-marker); toluene (2); ethyl benzene (3); propyl benzene (4); butyl benzene (5); pentyl benzene (6); hexyl benzene (7)

studies focused on the incorporation of nanomaterials to methacrylate-based monoliths [28, 29].

Regarding retention factor (*k*), as shown in Table 2, by increasing the amount of MCM-41 particles incorporated into the monolith up to 5 wt%, the *k*-values obtained for the alkylbenzenes increased. The enhanced retention is suggested to be due to the higher surface area of the composite matrix over the parent monolith. However, an increase in the amount of MCM-41 (from 10 to 25 wt%) into the polymer system caused some reduction in the *k*-values; whereas a further increase in the MCM-41 content (up to 35 wt%) provided more retentive monoliths. This behavior was explained due to changes in the polymerization mixture, which may induce not only changes in hydrophobicity (by diluting the BMA content) but also in monolith structure. The increase retention observed for the addition of a greater amount of MCM-41 microparticles was attributed to a larger proportion of these particles located near the outer surface of the polymer structure, giving hybrid monoliths with larger surface roughness (see protuberances on the globule surface, Fig. 1E), thus explaining the retention behavior observed.

As it can be seen in Table 2, the hybrid monoliths with embedded MCM-41 also showed higher efficiencies than the control monolith. Within these hybrid monoliths, the column prepared with 35 wt% MCM-41 showed the largest retention and efficiency (up to 58,400 plates m^{-1}) for alkyl benzenes (see Fig. 2 and Table 2).

The separation of alkyl benzenes was also tested using hybrid monoliths with embedded UVM-7 NPs under the same conditions as those used for MCM-41 material. As shown in Fig. 2, the hybrid stationary phases containing UVM-7 material also provided an increase in retention time for alkyl

Table 2 Retention factor (*k*) and efficiency (plates m^{-1}) for some alkyl benzenes using hybrid monoliths containing embedded MCM-41 and UVM-7[a]

	MSPs (wt%)	*u* (mm s^{-1})	Toluene		Propyl benzene		Hexyl benzene	
			k	*N* (m^{-1})	*k*	*N* (m^{-1})	*k*	*N* (m^{-1})
MCM-41	0.0	1.04	0.59	28,700	1.11	22,800	2.95	12,100
	2.0	0.91	0.66	49,000	1.21	39,300	3.15	33,500
	5.0	0.82	0.99	39,100	1.82	30,500	4.70	28,700
	10.0	0.35	0.78	40,900	1.45	39,500	3.75	20,900
	25.0	0.19	0.70	25,700	1.34	31,300	3.52	52,700
	35.0	0.16	1.00	33,200	1.91	42,700	5.18	58,400
UVM-7	1.0	0.83	0.60	46,600	1.11	38,100	2.85	32,300
	5.0	0.83	0.77	68,500	1.49	64,000	4.18	49,500
	10.0	0.56	0.95	30,300	1.76	20,800	4.79	19,600

[a] Working conditions as in Fig. 2

benzenes and EOF marker with increasing amount of embedded nanoparticles. In terms of *k*-values, an increase along UVM-7 percentage was observed which was ascribed to the presence of a large number of mesopores in the globular structures (see the rough surface of monoliths prepared with 10 wt% UVM-7, Fig. 1F compared with the control monolith, Fig. 1D).

Regarding the efficiency, hybrid monoliths prepared with a 5 wt% of UVM-7 showed the best efficiency for alkyl benzenes, reaching up to 68,500 plates m^{-1}.

A comparison of CEC performance of hybrid monoliths obtained with both types of MSPs was also accomplished. As it can be seen in Fig. 2, at a given MSP percentage, the addition of MCM-41 led to longer retention times accompanied with a peak broadening than that found by using UVM-7. These variations in separation performance were probably due to changes in the morphology of monolith in the presence of MCM-41 or UVM-7 related to differences in their particle size, pore size distribution and surface area (see Fig. S1 and Table 1). Thus, the MCM-41 type material shows an ordered framework and a narrow pore size distribution, whereas UVM-7 solids are characterized by a non-ordered (large) pore system. Consequently, these differences can influence on the swelling of particle surface by the growing nuclei and the posterior covering by polymer layers, giving as a result different morphological structures (see Fig 1E and F).

The performance of hybrid monolithic columns containing either MCM-41 or UVM-7 materials (Fig. 3) was also evaluated using a set of derivatives of benzoic acids. In this case, the pH of mobile phase was adjusted at 1.9 to avoid the ionization of most of these solutes (see pK_a values in Experimental section), and thus considering as relevant contribution to separation mechanism their hydrophobic interaction with the stationary phase.

As observed, an improved separation of benzoic acids was achieved for hybrid monoliths prepared with both MSPs compared to the control monolith. Moreover, the hybrid columns prepared with MCM-41 (at contents >25 wt%) (Fig. 3B) provided much better separation of benzoic acids than the columns containing embedded UVM-7 (Fig. 3C). Additionally, the column efficiency of MCM-41 incorporated monolith reached to 140,000 plates m^{-1} for 2-iodobenzoic acid.

Table 3 compares the characteristic features of our method with other recent mesoporous phases reported for the separation of small molecules. Thus, our efficiency values were comparable with those found in literature [31–34]; although were lower than the results reported using hybrid monoliths prepared

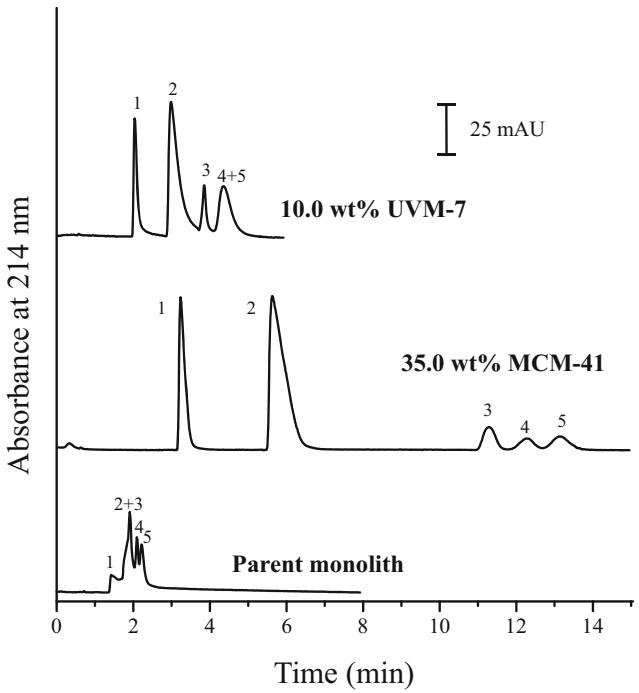

Fig. 3 CEC separation of a mixture of benzoic acids on control monolith and on hybrid monoliths containing 35 and 10 wt% of embedded MCM-41 or UVM-7 materials. Experimental conditions: mobile phase, 50:50 ACN:H_2O, 5 mM H_3PO_4, pH = 1.9; separation voltage, 15 kV; other details as in Fig. 2 Solutes: phthalic acid (1); salicylic acid (2); thiourea (3, EOF-marker); 2-iodobenzoic acid (4); benzoic acid (5)

Table 3 An overview on recently reported mesoporous phases for the separation of small molecules

Material	Analyte	Separation technique	Chromatographic mode	Efficiency (plates m^{-1})	Ref.
Poly(BMA-EDMA-Fe_3O_4@SiO_2/NH_2) and poly(BMA-EDMA-SBA-15/NH_2) monolithic columns	Benzoic acid derivatives	CEC	Mixed mode RP-AEX	24,000–290,000	[23]
Hybrid monolithic TEOS-APTES-with SBA-15	Thiourea, o-xylene, naphthalene and benzoic acid derivatives	CEC	Mixed mode	90,000–280,000	[24]
MCM-41-MPS incorporated monoliths	Phenol series, naphthyl substitutes, aniline series and alkyl benzenes	CEC	RP	157,000–209,000	[31]
Mesoporous SBA-15 silica rods	Thiourea, benzene, chlorobenzene, o-xylene, naphthalene	CEC	Mixed mode RP-IEX	110,000	[32]
MSP-C18-organo-silica monoliths	Alkyl benzenes	Capillary-LC	RP	95,000	[33]
Mesoporous organo-silica hybrid monoliths	Alkyl benzenes	nano-LC	RP	148,000	[34]
Poly(BMA-EDMA) with incorporated MCM-41 or UVM-7	Alkyl benzenes, cresols and benzoic acid derivatives	CEC	RP	69,000–140,000	Present work

TEOS tetraethoxysilane, APTES, 3-aminopropyltriethoxysilane, IEX ion exchange

with amino functionalized mesoporous wormlike SBA-15 rods [23] or modified with C18 groups [24]. However, our columns gave the most remarkable enhanced retention accompanied with a simple, fast and easy hybrid monolith preparation.

Also, the hybrid monoliths (prepared with both MSPs) were tested for the separation of positional isomers of cresols (Fig. S5). It was found that the hybrid columns prepared with MCM-41 (at 35 wt%) gave the best separation between *o*-cresol and *m*−/*p*-cresol peak.

In order to study changes in the separation mechanism of hybrid monolithic columns from apolar behaviour (RP phase) to a polar stationary phase through the embedding of hydrophilic silica (nano)particles, HILIC conditions were also tested. For this purpose, a test mixture containing thiourea and toluene was injected using a mobile phase with high contents of organic solvent (80:20 ACN:H_2O 5 mM H_3PO_4 pH = 2.5). Under RP conditions, thiourea elutes earlier than toluene. However, when the stationary phase is getting more polar (HILIC mode), the inversion of elution order of these analytes is produced [30]. However, the *k*-values obtained for toluene (measured from EOF marker) had positive values (data not shown); consequently, there was no inversion in retention order, in all synthesized hybrid monoliths with MSPs. This behavior supports our SEM observations on the modification induced by MSPs.

Finally, the hybrid monolith (with 35 wt% MCM-41) was successfully applied to the separation of acetylsalicylic and salicylic acids in analgesic formulation (Fig. S6). Both analytes were well separated and no interference from the matrix was detected.

Reproducibility of fabrication process

The reproducibility of the preparation protocol for hybrid monoliths with MSPs was tested. In particular, this study was performed for both hybrid monoliths containing embedded MCM-41 and UVM-7 materials. The run-to-run repeatability was evaluated from series of three injections of propyl benzene while the column-to-column reproducibility was estimated with three columns prepared from the same polymerization mixture. The batch-to-batch reproducibility was estimated from three batches of three columns each. As shown in Table S1, RSD values below 14.2% were found. Hence, the preparation protocol (described in Experimental Section) shows acceptable reproducibility and therefore avoiding sedimentation process even at higher contents of MSPs.

Conclusions

In this work, novel hybrid polymeric monoliths columns containing MSPs have been developed. These stationary phases were prepared by dispersing silica (nano)materials (MCM-41 or UVM-7) in the polymerization mixture before UV irradiation. Experimental preparation conditions were carefully optimized to assure homogenous distribution of the MSPs in the polymeric matrix with an additional stirring step during capillary filling. Thus, polymerization mixtures containing up to 10 wt% UVM-7 and 35 wt% MCM-41 were quite stable, showing negligible sedimentation during the short polymerization time used (15 min) in UV-initiation. To the best of our knowledge, such high contents of silica (nano)materials have not been employed in polymeric matrix to date.

The synthesized hybrid materials were applied to the CEC separation of test mixtures of alkyl benzenes, benzoic acid derivatives and cresols with enhanced retention compared to the control monolith. The higher retention observed for these solutes was probably due to the increase of the surface area of the resulting hybrid monoliths, produced by the presence of

MSPs. Satisfactory separations were generally obtained, although the baseline separation isomers was not fully achieved. Consequently, the prepared hybrid monoliths with these materials indeed played an outstanding effect in separation enhancement.

On the other hand, changes in the separation mode (from RP to HILIC), and consequently selectivity changes (elution order of thiourea and toluene) were not evidenced in the hybrid monoliths. This was attributed to that most of MSPs were embedded into the polymeric matrix.

Acknowledgements This work was supported by projects CTQ2014-52765-R and MAT2015-64139-C4-2-R (MINECO of Spain and Fondo Europeo de Desarrollo Regional, FEDER) and PROMETEO/2016/145 (Conselleria d'Educació, Investigació, Cultura i Esport, Generalitat Valenciana, Spain).

Compliance with ethical standards The author(s) declare that they have no competing interests.

References

1. Kresge KT, Leonowicz ME, Roth WJ, Vartuli JC, Beck JS (1992) Ordered mesoporous molecular sieves synthesized by a liquid-crystal template mechanism. Nature 359:710–712
2. Luque R, Balu AM, Campelo JM, Gracia MD, Losada E, Pineda A, Romero AA, Serrano-Ruiz JC (2012) Catalytic applications of mesoporous silica-based materials. Catalysis 24:253–280
3. Li Z, Barnes JC, Bosoy A, Stoddart JF, Zink JI (2012) Mesoporous silica nanoparticles in biomedical applications. Chem Soc Rev 41: 2590–2605
4. Walcarius A, Collinson MM (2009) Analytical chemistry with silica sol-gels: Traditional routes to new materials for chemical analysis. Annu Rev Anal Chem 2:121–143
5. Trewyn BG, Slowing II, Giri S, Chen HT, Lin VSY (2007) Synthesis and functionalization of a mesoporous silica nanoparticle based on the sol-gel process and applications in controlled release. Acc Chem Res 40(9):846–853
6. Zhao D, Sun J, Li Q, Stucky GD (2000) Morphological control of highly ordered mesoporous silica SBA-15. Chem Mater 12:275–279
7. Rahmat N, Abdullah AZ, Mohamed AR (2010) A review: Mesoporous santa barbara amorphous-15, types, synthesis and its applications towards biorefinery production. Am J Appl Sci 7: 1579–1586
8. Gustafsson H, Thörn C, Holmberg K (2011) A comparison of lipase and trypsin encapsulated in mesoporous materials with varying pore sizes and pH conditions. Colloids Surf. B Biointerfaces 15: 464–471
9. Cabrera S, El Haskouri J, Guillem C, Latorre J, Beltrán A, Beltrán D, Marcos MD, Amoros P (2000) Generalised syntheses of ordered mesoporous oxides: the atrane route. Solid State Sci 2(4):405–420
10. El Haskouri J, Ortiz de Zárate D, Guillem C, Latorre J, Caldés M, Beltrán A, Beltrán D, Descalzo AB, Rodríguez G, Martínez-Mañez R, Marcos MD, Amorós P (2002) Silica-based powders and monoliths with bimodal pore systems. Chem Commun 4:330–331
11. El Haskouri J, Morales JM, Ortiz de Zárate D, Fernandez L, Latorre J, Guillem C, Beltrán A, Beltrán D, Amorós P (2008) Nanoparticulated silicas with bimodal porosity: chemical control of the pore sizes. Inorg Chem 47(18):8267–8277
12. Pérez-Cabero M, Hungría AB, Morales JM, Tortajada M, Ramón D, Moragues A, El Haskouri J, Beltrán A, Beltrán D, Amorós P (2012) Interconnected mesopores and high accessibility in UVM-7-like silicas. J Nanopart Res 14:1045–1048
13. Ros-Lis JV, Casasús R, Comes M, Coll C, Marcos MD, Martínez-Máñez R, Sancenón F, Soto J, Amorós P, El Haskouri J, Garró N, Rurack K (2008) A mesoporous 3D hybrid material with dual functionality for Hg^{2+} detection and adsorption. Chemistry 14(27): 8267–8278
14. Svec F (2012) Quest for organic polymer-based monolithic columns affording enhanced efficiency in high performance liquid chromatography separations of small molecules in isocratic mode. J Chromatogr A 1228:250–262
15. Svec F, Lv Y (2015) Advances and recent trends in the field of monolithic columns for chromatography. Anal Chem 87:250–273
16. Chen X, Tolley HD, Lee ML (2011) Monolithic capillary columns synthesized from a single phosphate-containing dimethacrylate monomer for cation-exchange chromatography of peptides and proteins. J Chromatogr A 1218:4322–4331
17. Tasfiyati AN, Iftitah ED, Sakti SP, Sabarudin A (2016) Evaluation of glycidyl methacrylate-based monolith functionalized with weak anion exchange moiety inside 0.5 mm i.d. column for liquid chromatographic separation of DNA. Anal Chem Res 7:9–16
18. Lämmerhofer M, Gargano A (2010) Monoliths with chiral surface functionalization for enantioselective capillary electrochromatography. J Pharmaceut Biomed Anal 53:1091–1123
19. Acquah C, Obeng EM, Agyei D, Ongkudon CM, Moy CKS, Danquah MK (2017) Nano-doped monolithic materials for molecular separation. Separations 4:2–22
20. Navarro-Pascual-Ahuir M, Lucena R, Cárdenas S, Ramis-Ramos G, Valcárcel M, Herrero-Martínez JM (2014) UV-polymerized butyl methacrylate monoliths with embedded carboxylic single-walled carbon nanotubes for CEC applications. Anal Bioanal Chem 406:6329–6336
21. Zhang LS, Gao SP, Huang YP, Liu ZS (2016) Green synthesis of polymer monoliths incorporated with carbon nanotubes in room temperature ionic liquid and deep eutectic solvents. Talanta 154: 335–340
22. Navarro-Pascual-Ahuir M, Lerma-García MJ, Ramis-Ramos G, Simó-Alfonso EF, Herrero-Martínez JM (2013) Preparation and evaluation of lauryl methacrylate monoliths with embedded silver nanoparticles for capillary electrochromatography. Electrophoresis 34:925–934
23. Lei W, Zhang LY, Wan L, Shi BF, Wang YQ, Zhang WB (2012) Hybrid monolithic columns with nanoparticles incorporated for capillary electrochromatography. J Chromatogr A 1239:67–71
24. Wan L, Zhang L, Lei W, Zhu Y, Zhang W, Wang Y (2012) Novel hybrid organic-inorganic monolithic column containing mesoporous nanoparticles for capillary electrochromatography. Talanta 98:277–281
25. Liu Y, Chen Y, Yang H, Nie L, Yao S (2013) Cage-like silica nanoparticles-functionalized silica hybrid monolith for high performance capillary electrochromatography via "one-pot" process. J Chromatogr A 1283:132–139
26. Serjeant EP, Dempsey B (1979) Ionization constants of organic acids in aqueous solution, Pergamon
27. Peters EC, Petro M, Svec F, Fréchet JMJ (1998) Molded Rigid Polymer Monoliths as Separation Media for Capillary Electrochromatography. 1. Fine Control of Porous Properties and Surface Chemistry. Anal Chem 70:2288–2295
28. Huang HY, Lin CL, Wu CY, Cheng YJ, Lin CH (2013) Metal organic framework-organic polymer monolith stationary phases for capillary electrochromatography and nano-liquid chromatography. Anal Chim Acta 779:96–103
29. Carrasco-Correa EJ, Ramis-Ramos G, Herrero-Martínez JM (2015) Hybrid methacrylate monolithic columns containing magnetic

nanoparticles for capillary electrochromatography. J Chromatogr A 1385:77–84

30. Jiang Z, Reilly J, Brian E, Smith NW (2009) Novel zwitterionic polyphosphorylcholine monolithic column for hydrophilic interaction chromatography. J Chromatogr A 1216:2439–2448
31. Zhang L, Zhao Q, Li X, Li X, Huang Y, Liu Z (2016) Green synthesis of mesoporous molecular sieve incorporated monoliths using room temperature ionic liquid and deep eutectic solvents. Talanta 161:660–667
32. Zhang L, Wang Z, Zhang W (2013) Sub-micrometer mesoporous SBA-15 silica rods as stationary phase for capillary electrochromatography separation. Chin. J. Chromatogr 31(4):335–341
33. Liu S, Peng J, Liu Z, Liu Z, Zhang H, Wu R (2016) One-pot approach to prepare organo-silica hybrid capillary monolithic column with intact mesoporous silica particles as building block. Sci Rep 6:34718
34. Wu C, Liang Y, Yang K, Min Y, Liang Z, Zhang L, Zhang Y (2016) Clickable periodic mesoporous organosilica monolith for highly efficient capillary chromatographic separation. Anal Chem 88: 1521–1525